Changes in thermal conductivity, suction and microstructure of a compacted lime-treated silty soil during curing

Yejiao Wang, Yu-Jun Cui, Anh Minh A.M. Tang, Chaosheng Tang, Nadia Benahmed

Changes in thermal conductivity, suction and microstructure of a compacted lime-treated silty soil during curing

Yejiao WANG[1], Yujun CUI[1], Anh Minh TANG[1], Chaosheng TANG[2], Nadia BENAHMED[3]

[1]: Ecole des Ponts ParisTech, U.R. Navier/CERMES, 6 – 8 av. Blaise Pascal, Cité Descartes, Champs – sur – Marne, 77455 Marne – la – Vallée cedex 2, France

[2]: School of Earth Sciences and Engineering, Nanjing University, 163 Xianlin Road, Nanjing 210093, China

[3]: IRSTEA, Groupe de Recherche "Ouvrages hydrauliques", 3275 route Cézanne, CS 40061, 13182 Aix En Provence Cedex 5

Corresponding author:

Prof. Yu-Jun CUI

Ecole des Ponts ParisTech

6-8 av. Blaise Pascal, Cité Descartes, Champs-sur-Marne

F-77455 Marne – la – Vallée cedex - France

Telephone: +33 1 64 15 35 50

Fax: +33 1 64 15 35 62

E-mail: yu-jun.cui@enpc.fr

Abstract

An experimental study was conducted to investigate changes of thermal conductivity, suction and microstructure of a lime-treated silty soil during curing. The soil samples were prepared with 2% lime and compacted dry (17%) and wet (22%) of optimum. The thermal conductivity, total suction and pore size distribution were determined at various curing times. Results show that the thermal conductivity of samples compacted on the dry side decreases slightly with curing time, while the curing time effect on the samples compacted on the wet side is insignificant. The total suction generally increases with curing time even though the soil water content was kept constant. The pore size distribution characteristics are mainly related to its moulding water content. As the samples are compacted on the dry side, the pore size distribution shows typical bi-modal characteristics, with a population of macro-pores and a population of micro-pores. By contrast, as the samples are compacted on the wet side, the pore size distribution shows typical uni-modal characteristics. It is found that the modal size of both the large and small pores decreases with curing time.

Keywords: thermal conductivity; suction; microstructure; lime-treated soil; curing time; mercury intrusion porosimetry.

41 **INTRODUCTION**

42 Lime treatment is widely applied in geo-engineering constructions such as highway and
43 railway embankments, levees and slopes. This technique effectively improves the workability
44 and mechanical behaviour of soils, because lime can significantly modify soil properties
45 through a series of physical-chemical reactions, including hydration, cation exchanges and
46 pozzolanic reaction (Bell, 1996; Boardman et al. 2001; Prunsinski and Bhattacharja, 1999;
47 Umesha et al. 2009). Generally, lime hydration takes place shortly after adding lime into the
48 soil, and this process consumes a large amount of water. The main products of this first step
49 reaction is $Ca(OH)_2$. The followed ionization of hydration products provides sufficient Ca^{2+}
50 ions, and induces cation exchanges that lead to soil flocculation/agglomeration. Note that the
51 cation exchanges and the consequent flocculation process occur rapidly after lime addition,
52 resulting in changes in aggregate size distribution, plasticity and workability of soil (Bell,
53 1989; Russo, 2005). Pozzolanic reaction usually takes a longer time and plays the major role
54 in improving soil geotechnical behaviour, by increasing soil stiffness and shear strength (Bell,
55 1996; Consoli et al. 2009; Tang et al. 2011; Dong, 2013). Due to the time-dependence of
56 lime-soil reactions, the geotechnical behaviour of lime-treated soil depends significantly on
57 curing time (Locat et al. 1990; Bell, 1996; Little, 1999; AL-Mukhtar et al. 2012; DI Sante et
58 al. 2014). Brandl (1981) and Liu et al. (2012) reported that the strength of lime-treated soil
59 increased with increasing curing time. By performing bender element tests on lime-treated
60 soils, Dong (2013) showed that there was a two-stage development for the shear modulus
61 over time: stage 1 related to cation exchanges and stage 2 to pozzolanic reaction.

62 In most cases, lime-treated soils are exposed to natural environment or placed in shallow

63 depth. They are unavoidably subjected to long-term cyclic climate loadings, i.e. temperature
64 variations, drying and wetting, which can significantly affect their durability. Recent studies
65 mainly focus on the effect of wetting and drying cycles on the mechanical behaviour of
66 lime-treated soil (Khattab et al. 2007; Cuisinier and Deneele, 2008; Le Runigo, 2008; Tang et
67 al. 2011), and little attention has been paid to the effect of temperature, which is also an
68 important factor related to climate. Actually, temperature can also significantly affect the
69 geotechnical properties of soil, such as Atterberg limits, stiffness, strength and volume change
70 behaviour (Ctori, 1989; De Bruyn and Thimus, 1996; Sultan et al. 2002; Liu et al. 2012; Islam
71 et al. 2013; Consoli et al. 2014). To assess the temperature effect, it appears essential to
72 investigate soil thermal properties like thermal conductivity. Indeed, thermal conductivity is
73 an important parameter in the modelling of the coupled thermo-hydro-mechanical behaviour
74 of lime-treated soil under climate changes. It takes an important role in the heat
75 transformation between the soil and the atmospheric air. However, most studies on thermal
76 behaviour of treated soil involved cement stabilization in the past decades. Farouki (1981)
77 reported that the addition of Portland cement into sand increased the thermal conductivity of
78 the mixture in both wet and dry states. Adam and Jones (1995) observed that the thermal
79 conductivity of cement stabilized soil was higher than that of lime-stabilized soil, and they
80 explained that the former enhanced soil density while the later reduced it. Nevertheless,
81 El-Rawi and Al-Wash (1995) indicated that the thermal conductivities of both soil-cement
82 mixture and concrete decreased with curing time. Lee et al. (2014) tested the mixtures of the
83 gold tailings and fly ash, showing a decrease of thermal conductivity of the mixtures with
84 curing time. From these studies, it appears that the changes in thermal conductivity of

85 lime-treated soil and especially the effect of curing time have not been well understood yet.

86 Due to the climate effect, field lime-treated soils are usually at unsaturated state. Thus,
87 suction is a basic parameter to describe the state of soil-water-air system. For lime-treated
88 soils, it was found that the cation exchanges and the induced flocculation can modify the
89 water retention capacity of soil. Russo (2005), Tedesco and Russo (2008) observed an
90 increase in water retention capacity by lime addition. Russo (2005), Cecconi and Russo (2008)
91 attributed this phenomenon to the reduced interconnection between pores. Khattab et al. (2002)
92 compared the water retention curve of a lime-treated clay with that of untreated one, and
93 showed that the small increase of suction for the treated clay was due to water consumption
94 by lime hydration. In longer term, pozzolanic reaction becomes dominant in lime-treated soils,
95 creating cementitious compounds and giving rise to the modification of both microstructure
96 and water retention capacity of soil.

97 To better understand the observed macroscopic behaviour of soil such as thermal conductivity,
98 water retention capacity and stiffness, it is often required to perform soil microstructure
99 investigation. Mercury intrusion porosimetry (MIP) is one of the most widely used techniques
100 for this purpose. For lime-treated soils, due to the time-dependence of lime-soil interactions,
101 their microstructure is time-dependent. Russo et al. (2007) performed MIP tests on
102 lime-treated silt cured at different times, and highlighted the time-dependency of
103 microstructure changes: the cation exchanges and pozzolanic reaction reduced the porosity
104 and increased the quantity of small pores. Khattab et al. (2007) also studied the microstructure
105 changes of a lime-treated expansive soil under wetting/drying cycles, and found that the total
106 pore volume of treated soil increased drastically with wetting/drying cycles.

107 The above-mentioned studies show that different soil properties have been investigated for
108 different cement/lime-treated soils, and there is no study on different soil properties with a
109 fixed soil and a fixed treatment. This appears however essential to well understand different
110 mechanisms involved in the treatment processes. In this study, the changes of thermal
111 conductivity, suction and microstructure of a lime-treated unsaturated silty soil were analysed
112 during curing time. Two groups of soil samples were prepared at dry and wet sides of
113 optimum. The thermal conductivity, water retention capacity and pore size distribution of the
114 samples at various curing times (from 1 to 90 days) were determined. Results allowed the
115 coupled thermo-hydro-mechanical behaviour and the microstructure characteristics to be
116 analysed.

117 **MATERIALS AND METHODS**

118 *Test materials*

119 The soil tested was taken from a site near Héricourt, France. This soil has a fine fraction (< 80
120 μm) of 65 %. Its geotechnical properties are reported in Table 1. According to
121 French/European standard NF P 11-300 (1992), this soil belongs to category A2. It
122 corresponds to a silt of high plasticity (MH) following the Unified Soil Classification System
123 (USCS). The main minerals are quartz (55%), kaolinite (12%), feldspaths (11%), illite (10%),
124 goethite (6.5%), montmorillonite (4%), chlorite (1%) and rutile (0.5%) (Deneele & Lemaire,
125 2012). In Figure 1, both grain size distribution of natural soil and aggregate size distribution
126 of soil powder used in this study are presented. The grain size distribution was obtained on
127 the natural soil by the wet sieving method (NF P 94-056, for particles larger than 80 μm, and
128 by the hydrometer method (NF P 94-057, for particles smaller than 80 μm). Natural soil was

129 first air-dried, ground and then passed through the target sieve of 0.4 mm (D_{max}). The larger
130 soil aggregates which could not pass through this sieve were ground again, until all soil
131 passed through (Tang et al. 2011). Then the "aggregate size distribution" was determined by
132 dry sieving method.

133 Quicklime was used as additive. It is the same lime used in the embankment construction at
134 Héricourt, France. The main properties of this lime are presented in Table 2. In accordance
135 with the lime treatment in the embankment construction at Héricourt, 2 % lime by dry weight
136 of soil was chosen as the lime dosage.

137 *Sample preparation*

138 After the soil powder was prepared (D_{max} = 0.4 mm), 2% quicklime powder was first mixed
139 with dry soil. Then the soil-lime mixture was humidified by distilled water to reach different
140 target water contents. According to the compaction curves of lime-treated soil determined
141 from standard Proctor test (NF P 94-093, 1999) in Figure 2 (where the curve of untreated soil
142 is also shown), both the dry side (w_{dry} = 17%) and the wet side of optimum water content
143 (w_{wet} = 22 %) with the same dry density (ρ_d = 1.65 Mg/m^3) were considered. The water
144 contents and dry density were chosen according to the values applied in the field for the
145 embankment construction in Héricourt, France. After a mellowing period of 1 hour, static
146 compaction by 3 layers was performed to reconstitute the samples at the target dry density
147 and different sizes to satisfy the requirements of different tests. For instance, the samples for
148 thermal conductivity test had 50 mm in diameter and 75 mm in height; the samples for suction
149 measurement had 38 mm in diameter and 100 mm in height; the samples for MIP test had 50
150 mm in diameter and 20 mm in height. Immediately after compaction, sample was carefully

covered by plastic membrane and wrapped in a film. Then the sample was enveloped by scotch tape, confined in a hermetic box and cured in a chamber at a relative humidity of 100% and a temperature of 20±2°C.

Thermal conductivity tests

A thermal properties analyzer, KD2 (Decagon Devices Inc.) was used to measure the thermal conductivity of samples. Its principle is based on the transient hot-wire method. The thermal probe is a single-needle (KS-1) with a size of 1.3 mm diameter and 60 mm length. Its accuracy is 5% and the measurement range is 0.02 - 2 W/mK. This device meets the requirements of ASTM Standards (ASTM D5334-00, 2000). In order to install the thermal probe into the soil, a hole of 1.3 mm diameter and 60 mm depth was drilled in the centre of each compacted sample. As shown in Figure 3, a layer of thermal grease was first applied on the surface of the probe to ensure a good contact between the soil and the probe. Then, the thermal probe was installed inside of the soil sample. Before starting the measurement, about 10 min was needed for the temperature inside of the sample reaching stability. After that, the measurement was started by pressing the key “Enter” on the device. It took about 1 - 2 min for one measurement. Note that the measurement was performed in the laboratory at a temperature of 20±2°C. This measurement was being conducted during the whole curing time of t = 90 days for each soil sample.

Suction measurement

Once the samples were compacted, they were covered in watertight plastic films and stored for 24 h for water homogenization. Then the samples were cut into 6 or 8 small pieces (38

mm in diameter and 8 mm in height) which were well covered to prevent water evaporation during curing time. At a given curing time, one small piece was put into the dew point PotentiaMeter (WP4) to measure its suction. Immediately after the suction measurement, the water content was determined by oven-drying.

The dew point PotentiaMeter (WP4) measures the total suction in a sample. The total suction (ψ) of the sample was determined through Kelvin's equation:

$$\psi = \frac{RT}{M} \ln RH \quad (1)$$

where R is the gas constant (8.31 J/mol K), T is the Kelvin temperature of the sample, M is the molecular mass of water, RH is the relative humidity.

As RH is dependent on temperature (Tang and Cui, 2005), it is important to measure the temperature for each RH measurement. In the dew point PotentiaMeter, the dew point temperature of air is measured by a dew point sensor and the sample temperature is measured by an infrared thermometer.

Microstructure investigation

For the MIP tests, one small piece (around 1.1 g of dry soil) was cut carefully from the compacted sample (50 mm in diameter and 20 mm in height) at a certain curing time (t = 1, 28 and 90 days). Each small piece was freeze-dried immediately following the procedure proposed by Delage and Pellerin (1984), and then subjected to MIP test. Autopore IV 9500 mercury intrusion porosimeter which has both low-pressure and high-pressure systems was used. The pressure started from a value of 3 to 4 kPa in the low- pressure part up to around 230 MPa in the high-pressure part. With increasing pressure, mercury gradually intruded into

193 the sample starting from a maximum entry diameter of 355 μm to a minimum value of 0.006
194 μm according to Laplace's law:

195 $$p = \sigma \cos\theta \left(\frac{1}{r_1} + \frac{1}{r_2} \right) \quad (2)$$

196 where r_1 and r_2 are the curvature radii - in the case of spherical interface, $r_1 = r_2$; σ is the
197 surface tension (taken equal to 0.485 N/m); θ is the contact angle (taken equal to 130°); p is
198 the applied pressure.

199 Since the mercury cumulative intrusion can be assimilated to the air intrusion process, the
200 following equation can be deduced:

201 $$d = -\frac{4\sigma_m \cos\theta_m}{p_m} = \frac{4\sigma_w \cos\theta_w}{p_w} \quad (3)$$

202 where d is the diameter of intruded pore (assumed to be cylindrical), σ is the surface tension, θ
203 is the contact angle, p is the intrusion pressure, subscript m denotes mercury while subscript w
204 denotes water. In this study, the following values were taken: σ_m = 0.485 N/m, σ_w = 0.073
205 N/m, θ_m = 130° and θ_w = 0°.

206 The relationship between matric suction (u_a - u_w) and mercury intrusion pressure p_m can be
207 deduced from Eq. (3):

208 $$\left(u_a - u_w\right) = -\frac{\sigma_w \cos\theta_w}{\sigma_m \cos\theta_m} p_m \quad (4)$$

209 The water content w and degree of saturation S_r can be determined using the following
210 equations by considering the residual water content w_r (Romero, 1999):

211 $$w = \left(1 - S_{rm}\right)\left(w_{sat} - w_r\right) + w_r \quad (5)$$

212 $$S_r = (1 - S_{rm}) + \frac{w_r}{w_{sat}} S_{rm} \quad (6)$$

213 where S_{rm} is the degree of saturation of mercury, w_{sat} is the water content at saturation.

214

215 **EXPERIMENTAL RESULTS**

216 *Thermal conductivity tests*

217 Figure 4 shows the thermal conductivity of lime-treated samples versus curing time on a
218 semi-logarithmic scale. It can be seen that, for the samples compacted on the wet side, the
219 curing effect on the thermal conductivity is negligible, the value remaining around 1.50
220 W/mK. For the samples compacted on the dry side, the thermal conductivity decreases
221 slightly during curing. At t = 1 day, the thermal conductivity is about 1.36 W/mK; it decreases
222 by 5.1% to about 1.29 W/mK at t = 90 days. The decreasing thermal conductivity with curing
223 time was also reported for soil-cement mixture and concrete (El-Rawi and Al-Wash, 1995),
224 gold tailings and fly ash mixtures (Lee et al. 2014), cement paste (Hansen et al, 1982).
225 Mojumdar et al. (2006) measured the thermal conductivity of synthetic calcium silicate
226 hydrate (C-S-H), the main cementitious product of lime treatment, and a value of 0.1012
227 W/mK at 25°C was found. Note that the value for water is 0.6 W/mK, much higher than that
228 of C-S-H (Van Wijk, 1963; Farouki, 1981). This explains why wet samples (w = 22%) always
229 have higher thermal conductivity than the dry samples (w = 17%).

230 *Suction measurement*

231 The suction variations with curing time are shown in Figure 5a. As expected, at given curing

232 time, the suction of dry side samples (w = 17 %) is generally higher than that of wet side
233 samples (w = 22%). It is also observed that the suction of all samples increases with curing
234 time. For the samples compacted dry of optimum, the suction is 270 kPa at t = 2 days; then it
235 gradually increases to 500 kPa at t = 90 days. Similarly, for the samples compacted wet of
236 optimum, the suction increases from 170 kPa at t = 4 days to 300 kPa at t = 90 days.
237 Interestingly, these suction changes occur in almost constant water content conditions. Indeed,
238 Figure 5b shows that the measured water contents remain almost constant with curing time:
239 the water content of the wet side samples is about 22 %, and that of dry samples is about 17 %
240 during the whole curing time. Note that the dry density was monitored during curing and a
241 variation of 0.119 - 0.850% was recorded. This variation is very small and its effect on
242 suction changes can be ignored. It can be deduced that the lime treatment increases the water
243 retention capacity of soils. This is consistent with the observations made by Russo (2005),
244 Cecconi and Russo (2008), and Tedesco (2007), suggesting that the water retention capacity
245 of lime-treated soils is improved over time.

246 *Microstructure investigation*

247 The derived curves and the corresponding cumulative curves are presented in Figure 6 for the
248 samples compacted on dry side, and in Figure 7 for the samples compacted on wet side. It is
249 observed that the derived curves of the samples compacted on dry side (Figure 6a) show
250 typical bi-modal characteristics, indicating the presence of two populations of pores:
251 macro-pores and micro-pores, while the samples compacted on the wet side illustrate typical
252 uni-modal characteristics, indicating the presence of only one population of pores (Figure 7a).
253 These observations are in agreement with those of Delage et al. (1996) on compacted silt and

254 Russo et al. (2007) on lime-treated silt. In Figure 6a, each curve corresponds to a curing time
255 (t = 1, 28, and 90 days). It appears that the average entry diameters of both macro-pores and
256 micro-pores slightly decrease with curing time. Specifically, the size of macro-pores
257 decreases from 5.27 μm to 4.18 μm after 90 day curing; for the population of micro-pores, its
258 modal size also decreases from 0.23 μm to 0.07 μm after 90 curing days. Similar results are
259 obtained on the samples compacted on wet side. The single peak of pores shifts from 0.28 μm
260 at 1 day to 0.13 μm at 90 days (Figure 7a).

261 The cumulative curves are plotted in a semi-logarithmic scale, in terms of mercury intruded
262 void ratio as a function of entrance pore diameter as indicated in Figure 6b and Figure 7b.
263 With curing time, the final intrusion void ratio of the samples compacted on the wet side
264 continues to decrease and does not stabilize (Figure 7b); this decrease is more obvious for the
265 samples compacted on dry side (Figure 6b).

266 According to the pore size distribution curves shown in Figure 6a and Figure 7a, the water
267 retention curves can be determined as explained in section Materials and Methods, and they
268 are presented in Figure 8. Note that the suction determined from MIP curve corresponds to
269 capillary suction or matric suction. The corresponding measured total suction values are also
270 presented for comparison. On the dry side, at w = 17% (Figure 8a), the matric suction
271 obtained from the curves increases from about 400 to about 1000 kPa when the curing time
272 increases from 1 to 90 days. Similarly, on the wet side, at w = 22% (Figure 8b), the matric
273 suction also increases from about 180 to 300 kPa when the curing time increases from 1 to 90
274 days. In comparison with the direct measurements, the matric suction seems to be higher than
275 the total suction – the direct measurement points are located beneath the curves from the MIP

276 tests. This seems to be weird and will be discussed in the following section. On the whole,
277 both the direct and indirect measurement data illustrate that the water retention capacity of
278 lime-treated samples is improved gradually with curing time. This is in good agreement with
279 the results of Russo (2005), Cecconi and Russo (2008), and Tedesco (2007).

280 **DISCUSSION**

281 Soil effective thermal conductivity is significantly controlled by the volumetric components.
282 Generally, soil consists of solid particles which contain various minerals with different
283 thermal properties. They are surrounded by pore-air and pore-water. It was reported that the
284 thermal conductivity of most soil minerals is around 2.7 W/mK (Farouki, 1981). However,
285 the thermal conductivity value of the main hydration product (C-S-H) of lime is 0.1012
286 W/mK, much lower than that of water (0.6 W/mK) (Mojumdar et al. 2006; Farouki, 1981).
287 Thus, the presence of pozzolanic products during curing decreases the effective thermal
288 conductivity of the whole system.

289 Soil thermal conductivity also significantly depends on soil structure defined by soil porosity,
290 pore size distribution, particle contacts, etc. In general, soil compacted at different water
291 contents presents different microstructures (Delage et al. 1996). As shown in Figure 6 and
292 Figure 7, the soil compacted dry of optimum (degree of saturation of about 67%) presents
293 aggregated structure with large macro-pores, which are usually filled with continuous air
294 phase and discontinuous water phase in case of low degree of saturation, most water being in
295 the small pores inside the aggregates. By contrast, the soil compacted wet of optimum (degree
296 of saturation of about 87%) presents a dispersed structure with continuous water phase in the
297 pores and air phase in mostly occluded state (Delage et al. 1996; Wroth and Houlsby, 1985;

298 Alonso et al. 1987; Tedesco, 2007). These two different microstructures result in different
299 thermal contacts among soil grains. It is therefore reasonable that the thermal conductivity of
300 lime-treated soil is largely dependent on its initial compaction water content as shown by the
301 results in Figure 4. On the dry side, the thermal conductivity of samples is dominated by the
302 solid contacts between aggregates. But because in this case the macro-pores are filled with
303 continuous pore air and discontinuous pore water, the thermal conductivity is relatively lower.

304 The cementitious compounds mainly coat the surface of aggregates (Deneele et al., 2010), and
305 therefore modify the thermal contact conditions. Due to the relative low thermal conductivity
306 of cementitious compounds, the overall thermal conductivity of treated soil decreases with
307 increasing amount of cementitious compounds. As a result, the measured thermal
308 conductivity of dry side samples decreases with curing time (Figure 4). On the wet side, the
309 dispersed structure has more solid contacts between soil particles than aggregated structure of
310 dry side samples. Moreover, the liquid phase in pores is continuous and dominates the heat
311 transfer process in soil. As indicated above, the thermal conductivity of water is about 6 times
312 higher than cementitious compounds of lime. Consequently, the effect of cementitious
313 compounds on the overall thermal conductivity of soil becomes negligible. This explains the
314 observation in Figure 4 with the thermal conductivity of the wet side samples remaining
315 almost unchanged during curing.

316 The suction determined by both direct and indirect measurements increases over curing time
317 (Figure 8), while the water content dose not decrease (Figure 5). This is due to the fact that
318 water consumption of lime mainly takes place in the first step of hydration and becomes
319 negligible in the later pozzolanic reactions (Prusinski and Bhattacharja, 1999; Umesha et al.

320 2009). The increase of suction can be attributed to the pozzolanic reaction which changes the
321 soil microstructure. The results of MIP tests illustrate that the sizes of both macro-pores and
322 micro-pores decrease continuously with curing time (Figure 6 and Figure 7). To some extent,
323 the creation of cementitious compounds with a porous character would contribute to the
324 increase in the quantity of micro-pores (Cerny et al. 2006; Deneele et al. 2010). Besides, the
325 cementitious compounds are mainly coating on the surface of soil particles, blocking some
326 entrances of micro-pores and increasing the occluded pores. Furthermore, cementitious
327 products which occur at the clay edges, could bind the soil particles together, resulting in a
328 reduction of macro-pore size and modifying the interconnection of macro-pores. All these
329 changes would increase the water retention capacity of soil. As far as the difference of suction
330 between the direct measurement and the indirect measurement is concerned, the water
331 retention curves determined from MIP data correspond to the drying path, while the direct
332 measurement points corresponds to a state between the drying path and the wetting path –
333 they are located in a scanning curve. It is thereby logical to have the direct measurement
334 points below the curves from the MIP data (Figure 8).

335 **CONCLUSION**

336 A series of laboratory tests were performed on lime-treated silty soil samples compacted dry
337 and wet of optimum. Emphasis was put on the effects of curing time on thermal conductivity,
338 suction and microstructure. The obtained results allow the following conclusions to be drawn:

339 1) The samples compacted dry of optimum show typical bi-modal pore size distribution
340 characteristics, while the samples compacted wet of optimum show typical uni-modal
341 pore size distribution characteristics. With curing time, both the modal sizes of micro-

342 pores and macro-pores shift to lower values, due to the cementitious compounds produced
343 from pozzolanic reaction that fill the pores gradually over time.

344 2) The thermal conductivity of lime-treated soil over curing time significantly depends on
345 the moulding water content: for the samples compacted dry of optimum, the thermal
346 conductivity decreases slightly with increasing curing time; for the samples compacted
347 wet of optimum, the effect of curing time on the thermal conductivity is insignificant. The
348 slight decrease observed on dry side can be explained by the production of cementitious
349 compounds with lower thermal conductivity that coat the aggregates, slightly modifying
350 the thermal contact conditions over time. For the soil compacted wet of optimum, owing
351 to the dispersed structure which has more solid contacts and a continuous liquid phase in
352 pores, this effect of cementitious compounds becomes negligible.

353 3) Due to the modification of microstructure by the generation of cementitious compounds,
354 the suction of lime-treated soil generally increases with curing time, regardless of the
355 moulding water content.

356 The obtained results give an insight into the modifications of soil properties induced by lime
357 treatment during curing, helping better understand the curing effect on the evolutions of
358 thermal conductivity, suction and microstructure of the lime treated soil. These results can be
359 further used to analyse the thermo-hydro-mechanical behaviour of lime-treated soil. Moreover,
360 this study also provides useful elements to appreciate the durability of lime-stabilised soils. It
361 will be extended to other stabilised soils like lime-treated clay in order to verify the
362 conclusions drawn.

ACKNOWLEDGEMENTS

The authors wish to acknowledge the support of the European Commission via the Marie Curie IRSES project GREAT - Geotechnical and geological Responses to climate change: Exchanging Approaches and Technologies on a world-wide scale (FP7-PEOPLE-2013-IRSES- 612665). The support from China Scholarship Council (CSC) and Ecole des Ponts ParisTech are also gratefully acknowledged.

REFERENCES

Adams, E., Jones, P., 1995. Thermophysical properties of stabilised soil building blocks. Building and Environment 30 (2), 245-253

AL Mukhtar, M., Khattab, S., Alcover, J., 2012. Microstructure and geotechnical properties of lime-treated expansive clayey soil. Engineering Geology 139, 17-27.

Alonso E.E., Gens A., Hight D.W., 1987. Special problem soils-General report, IX ECSMFE. Dublin 3, 1087-1146.

ASTM D4373-02, 2007. Standard test method for rapid determination of carbonate content of soils. ASTM International, West Conshohocken, PA.

ASTM D5334-00, 2000. Standard test methods for determining of thermal conductivity of soil and soft rock by thermal needle probe procedure. ASTM International, West Conshohocken, PA.

383 Bell, F. G., 1989. Lime stabilisation of clay soils. Bulletin of the International Association of
384 Engineering Geology 39 (1), 67-74.

385 Bell, F. G., 1996. Lime stabilization of clay minerals and soils. Engineering Geology 42 (4),
386 223-237.

387 Boardman, D. I., Glendinning, S., Rogers, C. D. F., 2001. Development of stabilisation and
388 solidification in lime–clay mixes. Géotechnique 51 (6), 533-543.

389 Brandl, H., 1981. Alteration of soil parameters by stabilization with lime. In Proceedings of
390 the 10th International Conference on Soil Mechanics and Foundation Engineering. Vol.3,
391 Stockholm.

392 Cecconi, M., Russo, G., 2008. Prediction of soil-water retention properties of a lime stabilised
393 compacted silt. Unsaturated Soils: Advance in Geo-Engineering-Toll et al. (eds). Taylor &
394 Francis Group, London, ISBN 978-0-415-47692-8, 271-276.

395 Cerny, R., Kunca, A., Tydlitat, V., Drchalova, J., Rovnanikova. P., 2006. Effect of pozzolanic
396 admixtures on mechanical, thermal and hygric properties of lime plasters. Construction and
397 Building Materials 20(10), 849-857.

398 Consoli, N.C., Lopes, L.S., Heineck, K.S., 2009. Key parameters for the strength control of
399 lime stabilized soils. Journal of materials in Civil Engineering 21 (5), 210-216.

400 Consoli, N.C., Gravina da Rocha, C., Silvani, C., 2014. Effect of Curing Temperature on the
401 Strength of Sand. Coal Fly Ash, and Lime Blends, Journal of Materials in Civil Engineering
402 26 (8), 06014015.

403 Ctori, P., 1989. The effects of temperature on the physical properties of cohesive soil. Ground

Engineering 22 (5).

Cuisinier, O., Deneele, D., 2008. Impact of cyclic wetting and drying on the swelling properties of a lime-treated expansive clay. Jourées Nationales de Géotechnique et de Géologie de l'Ingénieur JNGG'08, Nantes, 18-20.

De Bruyn, D., Thimus, J., 1996. The influence of temperature on mechanical characteristics of Boom clay: the results of an initial laboratory programme. Engineering Geology 41 (1), 117-126.

Delage, P., Audiguier, M., Cui, Y. J., Howat, M., 1996. Microstructure of a compacted silt. Canadian Geotechnical Journal 33 (1), 150-158.

Delage, P., Marcial, D., Cui, Y. J., Ruiz, X., 2006. Ageing effects in a compacted bentonite: a microstructure approach. Géotechnique 56 (5), 291-304.

Delage, P., Pellerin, F.M., 1984. Influence de la lyophilisation sur la structure d'une argile sensible du Québec. Clay Minerals 19 (2), 151-160.

Deneele, D., Cuisinier, O., Hallaire, V. Masrouri, F., 2010. Microstructural evolution and physico-chemical behavior of compacted clayey soil submitted to an alkaline plume. Journal of Rock Mechanics and Geotechnical Engineering 2(2), 169-177.

Deneele, D., Lemaire, K., 2012. Evaluation de la durabilité des sols - Effet de la circulation d'eau sur la durabilité du limon traité_Approche multi - échelle, Livrables du projet TerDOUEST (Terrassement Durables – Ouvrages En Sols Traités, 2008-2012).

DI Sante, M., Fratalocchi, E., Mazzieri, F., 2014. Time of reactions in a lime treated clayey soil and influence of curing conditions on its microstructure and behaviour. Applied Clay

425 Science 99, 100-109.

426 Dong, J., 2013. Investigation of aggregates size effect on the stiffness of lime and/or cement
427 treated soil: from laboratory to field conditions. PhD Dissertation, Ecole Nationale des Ponts
428 et Chaussées, France.

429 EL Rawi, N., AL Wash, A., 1995. Strength and thermal properties of plain and reinforced
430 soil-cement. Journal of Islamic Academy of Sciences 8 (3), 107-118.

431 Farouki, O., 1981. Thermal properties of soils. Cold Regions Research and Engineering Lab
432 Hanover NH. Monograph, 81-1USA-CRREL.

433 Hansen, P.F., Hansen, J., Hougaard, K., Pedersen, E.J., 1982. Thermal properties of hardening
434 cement paste. Proceedings of RILEM International Conference on Concrete at Early Ages.
435 RILEM, Paris, 1982, 23-36.

436 Islam, S., Haque, A., Wilson, S.A., 2013. Effects of Curing Environment on the Strength and
437 Mineralogy of Lime-GGBS–Treated Acid Sulphate Soils. Journal of Materials in Civil
438 Engineering 26 (5), 1003-1008.

439 Khattab, S.A.A., AL-Mukhtar, M., Fleureau, J., 2002. Effect of initial suction on the swelling
440 pressure and porosity of lime stabilized clays. Unsaturated Soils. Swets & Zeitlinger, Lisse.
441 ISBN 90 5809 371 9, 605-609.

442 Khattab, S. A., Al-Mukhtzr, M., Fleureau, J. M., 2007. Long-term stability characteristics of a
443 lime-treated plastic soil. Journal of Materials in Civil Engineering 19 (4), 358-366.

444 Lee, J., Shang, J., Jeong, S., 2014. Thermo-mechanical properties and microfabric of fly
445 ash-stabilized gold tailings. Journal of Hazardous Materials 276, 323-331.

Le Runigo, B., 2008. Duability of the lime-treated Jossigeny silt under different hydraulic stresses: assessment of the mechanical, hydraulic microstructural, microstructural behavior, PhD thesis, Ecole Centrale de Nantes et Universite de Nantes.

Little, D.N., 1999. Evaluation of structural properties of lime stabilized soils and aggregates. Vol.1: Summary of Findings Prepared for the National Lime Association.

Liu, M.D., Indraratna, B., Horpibulsuk, S., 2012. Variations in strength of lime-treated soft clays. Proceedings of the ICE-Ground Improvement 165 (4), 217-223.

Locat, J., Bérubé, M.A., Choquette, M., 1990. Laboratory investigations on the lime stabilization of sensitive clays: shear strength development. Canadian Geotechnical Journal 27 (3), 294-304.

Mojumdar, S., Raki, L., Mathis, N., Schimdt, K., Lang, S. 2006. Thermal, spectral and AFM studies of calcium silicate hydrate-polymer nanocomposite material. Journal of thermal analysis and calorimetry 85 (1), 119-124.

NF P 11-300, 1992. Standard for classification of materials for use in the construction of embankments and capping layers of road infrastructures.

NF P 94-051, 1988. Standard test for soils investigation and testing-Determination of Atterberg's limites-Liquid limit test using Casagrande appraratus-Plasitic limit test on rolled thread.

NF P 94-054, 1991. Standard test for soils investigation and testing-Determination of particle density-Pycnometer method.

NF P 94-068, 1998. Standard test for soils investigation and testing-Measurement of the

467 methylene blue adsorption capacity of a rocky soil-Determination of the methylene blue of a
468 soil by means of the stain test.

469 NF P 94-093, 1999. Stanard test for soils investigation and testing-Determination of the
470 compaction characteristics of a soil-Standard Proctor test.

471 Prusinski, J. R., Bhattacharja, S., 1999. Effectiveness of Portland cement and lime in
472 stabilizing clay soils. Transportation Research Record: Journal of the Transportation Research
473 Board 1652 (1), 215-227.

474 Romero, E., 1999. Thermo-hydro-mechanical behaviour of unsaturated Boom clay: an
475 experimental study. PhD Thesis, Universidad Politécnica de Catalunya, Barcelona, Spain.

476 Russo, G., 2005. Water retention curves of lime stabilised soil. Advanced Experimental
477 Unsaturated Soil Mechanics. Taylor & Francis, London, 391-396.

478 Russo, G., Dal Vecchio, S., Mascolo, G., 2007. Microstructure of a lime stabilised compacted
479 silt. In Experimental Unsaturated Soil Mechanics, Springer Berlin Heidelberg, 49-56.

480 Sultan, N., Delage, P., Cui, Y., 2002. Temperature effects on the volume change behaviour of
481 Boom clay. Engineering Geology 64 (2), 135-145.

482 Tang, A., Cui, Y., 2005. Controlling suction by the vapour equilibrium technique at different
483 temperatures and its application in determining the water retention properties of MX80 clay.
484 Canadian Geotechnical Journal 42 (1), 287-296.

485 Tang, A., Vu, M., Cui, Y., 2011. Effects of the maximum grain size and cyclic wetting/drying
486 on the stiffness of a lime-treated clayey soil. Géotechnique 61, 421-429.

487 Tedesco, D.V., 2007. Hydro-mechanical behaviour of lime-stabilised soils. PhD Thesis,
488 University of Cassino, Italy.

489 Tedesco, D., Russo, G., 2008. Time dependency of the water retention properties of a lime
490 stabilised compacted soil. Unsaturated Soils: Advance in Geo-Engineering-Toll et al. (eds).
491 Taylor & Francis Group, London, ISBN 978-0-415-47692-8, 277-282.

492 Umesha, T., Dinesh, S., Sivapullaiah, P., 2009. Control of dispersivity of soil using lime and
493 cement. International Journal of Geology 3(1), 8-16.

494 Van Wijk, W., 1963. Physics of plant environment. Physics of Plant Environment.

495 Wroth C.P., Houlsby G.T., 1985. Soil mechanics: property characterization and analysis
496 procedure. Proc. of the XI ICSMFE, San Francisco (I), 1-55.

497

List of Tables

List of Figures

523

524 **Table 1 Geotechnical properties of the studied soil**

Property	Value
Specific gravity, G_s (NF P 94-054)	2.70
Liquid limit, w_L (%) (NF P 94-051)	51
Plastic limit, w_p (%) (NF P 94-051)	28
Plasticity Index, I_p (%) (NF P 94-051)	23
VBS (g/100g) (NF P 94-068)	2.19
$CaCO_3$ content (%) (ASTM D4373-02:2007)	1.4
Optimum moisture content (%) (NF P 94-093)	17.9
Maximum dry unit mass (Mg/m^3) (NF P 94-093)	1.76

525

526

527 **Table 2 Parameters of the used lime**

Chemical analysis	
CaO (%)	97.30
CaO + MgO (%)	98.26
MgO (%)	0.96
CO_2 (%)	0.25
SO_3 (%)	0.06
Aggregate size analysis	
≤ 80 μm (%)	82.7
≤ 200 μm (%)	95.2
≤ 2 mm (%)	100.0

528

529

530

531 **Figure 1 Aggregate size distribution of soil with D_{max} = 0.4 mm and grain size distribution of natural soil**

532

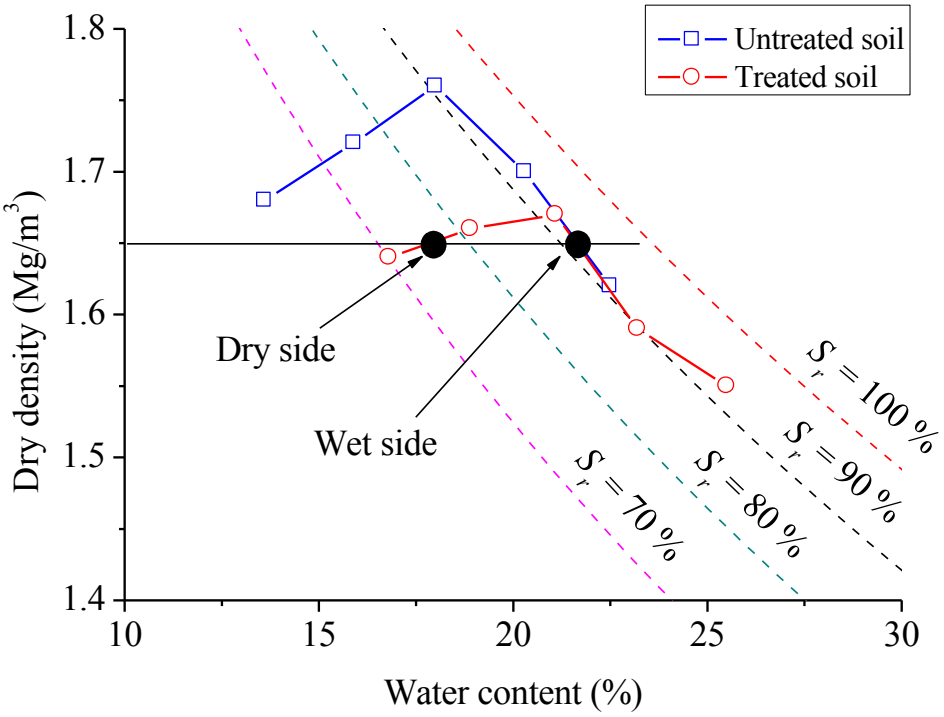

533

534 **Figure 2 Normal proctor curve of lime-treated silt (after Dong, 2013)**

535

536 (a)

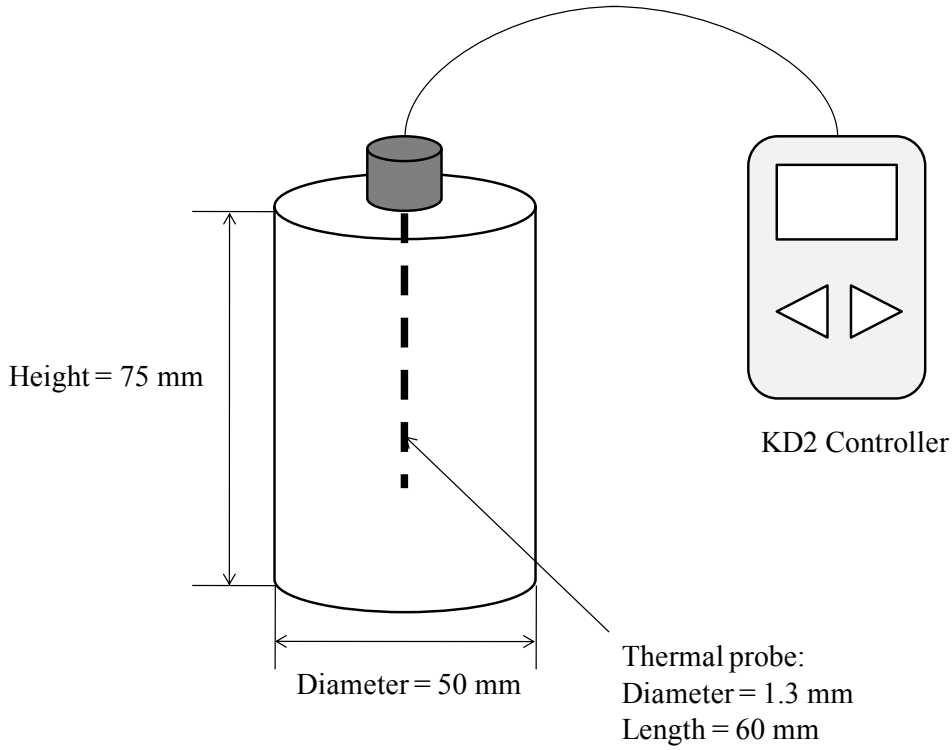

537

538 (b)

539

540 **Figure 3 Setup of thermal conductivity measurement: (a) sketch of setup; (b) photo of setup**

541

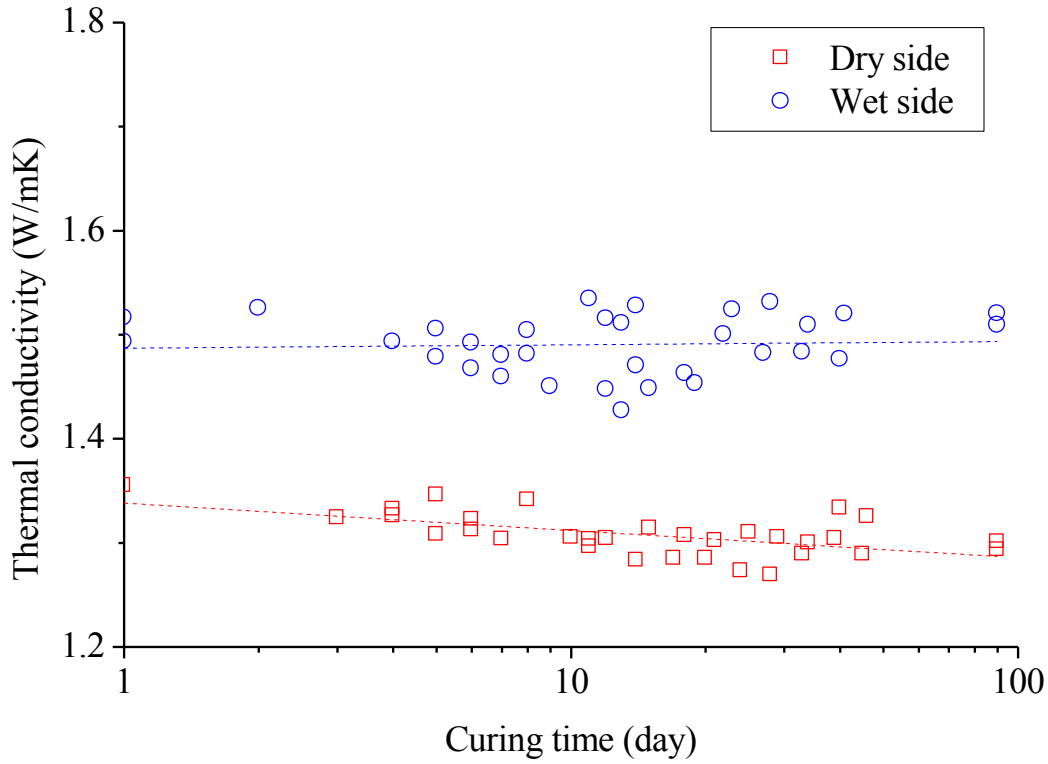

Figure 4 Thermal conductivity of lime-treated soil during curing time

a)

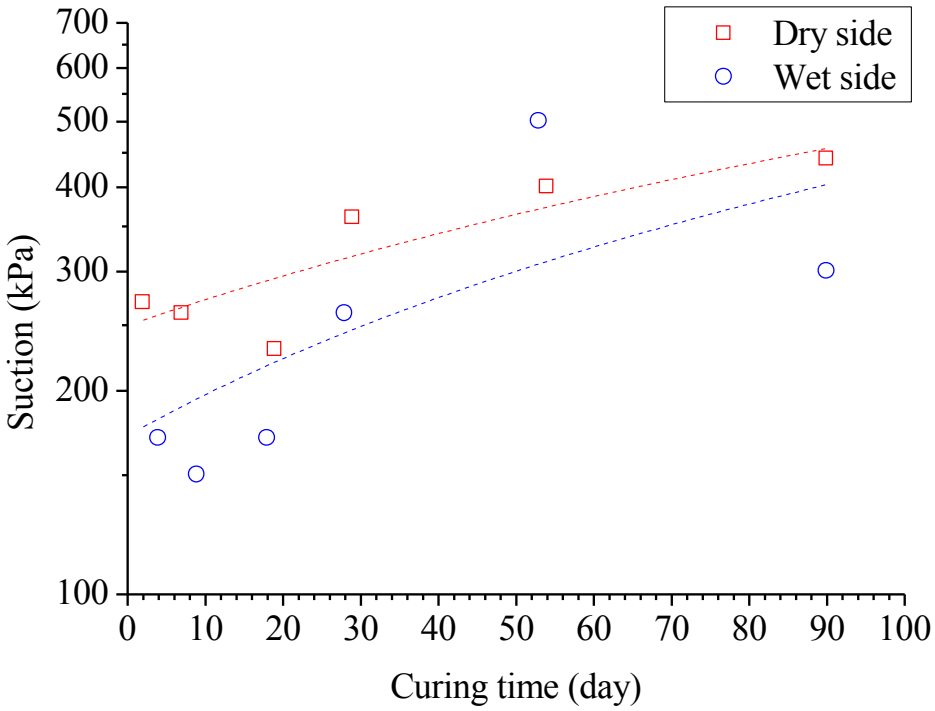

546

b)

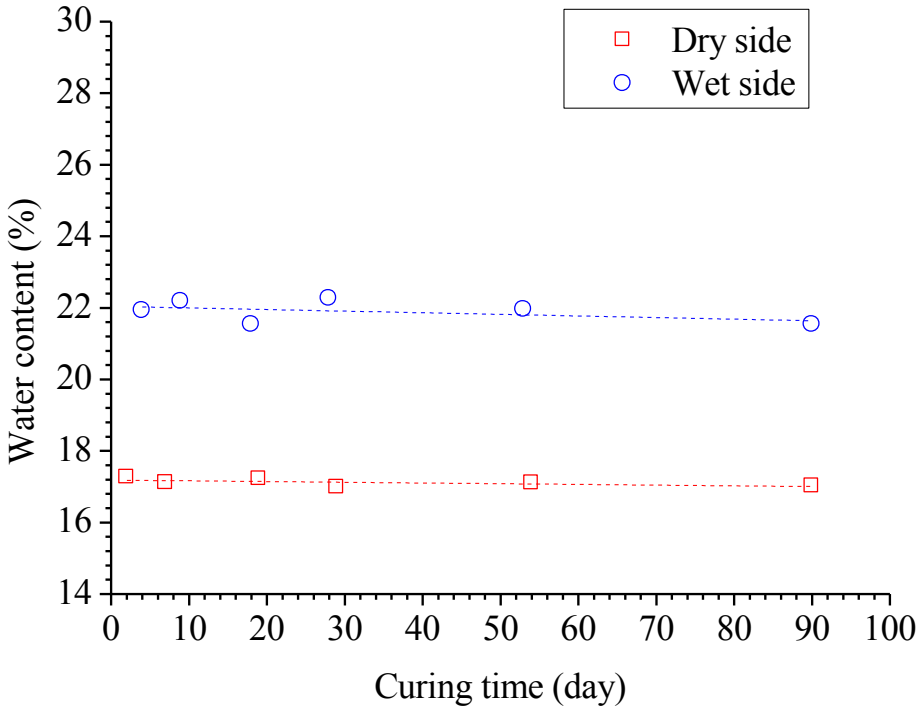

547

548 **Figure 5 (a) Suction changes of lime-treated soil during curing time and (b) water content variations of**
549 **lime-treated soil during curing time**

a)

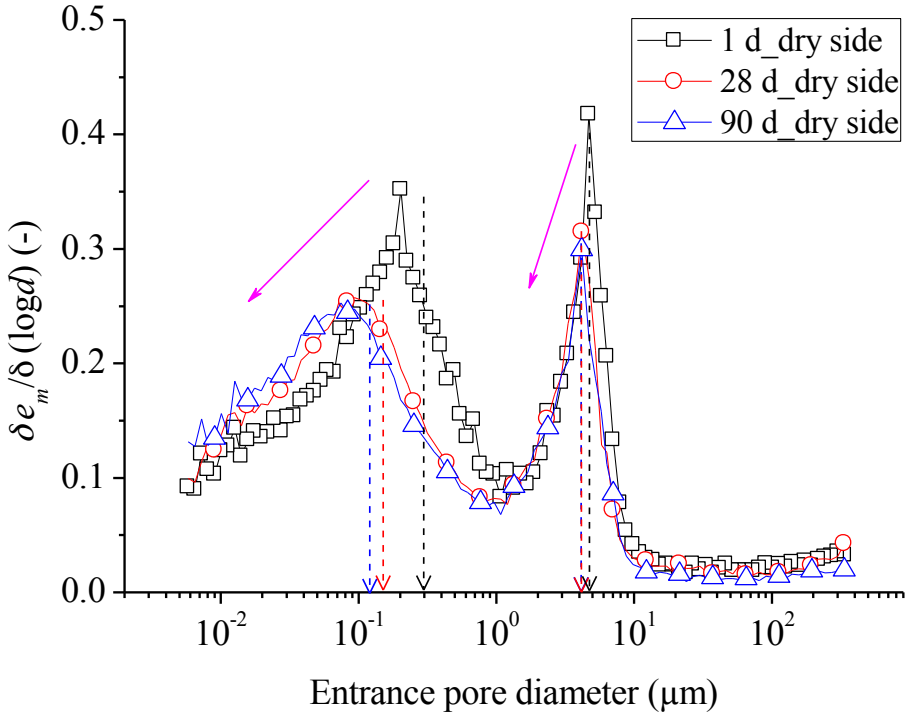

550

b)

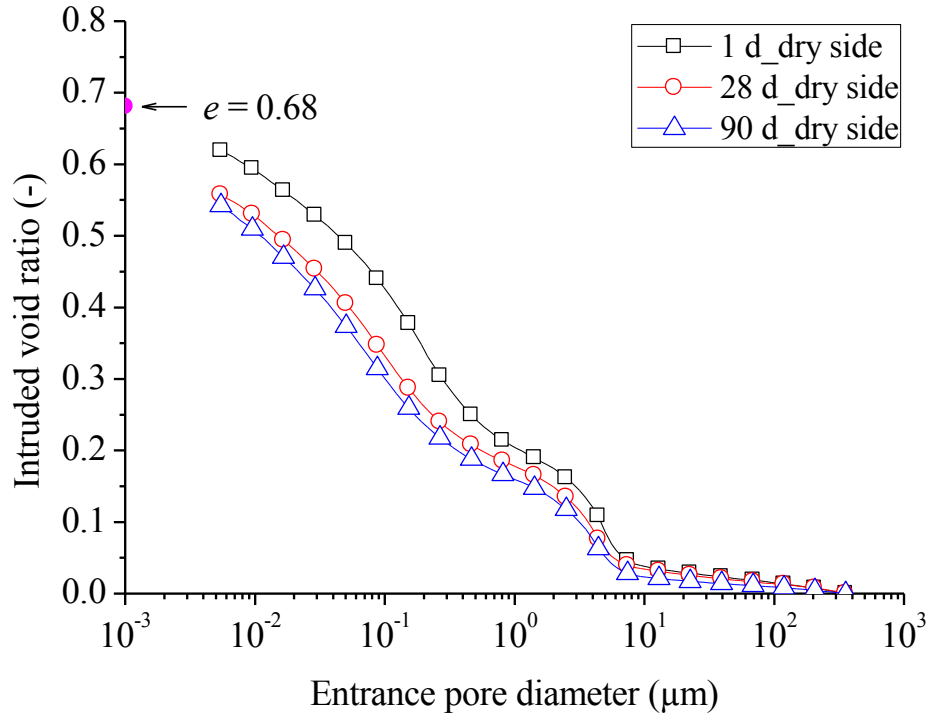

551

552 **Figure 6 (a) Derived pore size distribution curves of lime-treated samples compacted on the dry side and**
553 **(b) cumulative curves of lime-treated sample compacted on the dry side (e_m: mercury intruded void ratio;**
554 ***d*: entrance pore diameter and *e*: void ratio of the as-compacted sample)**

555

556

a)

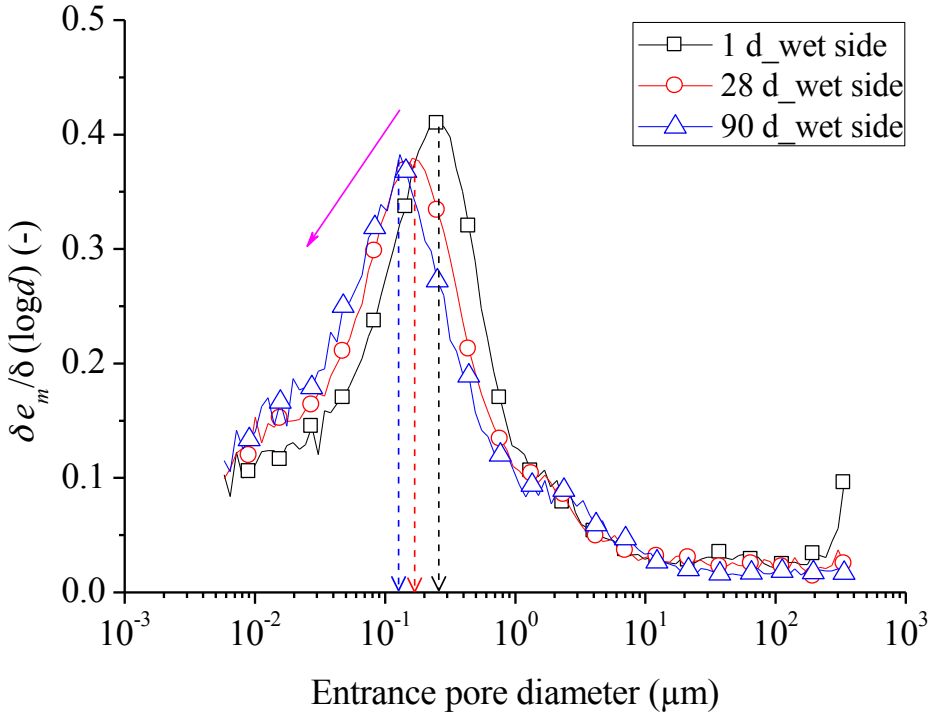

557

b)

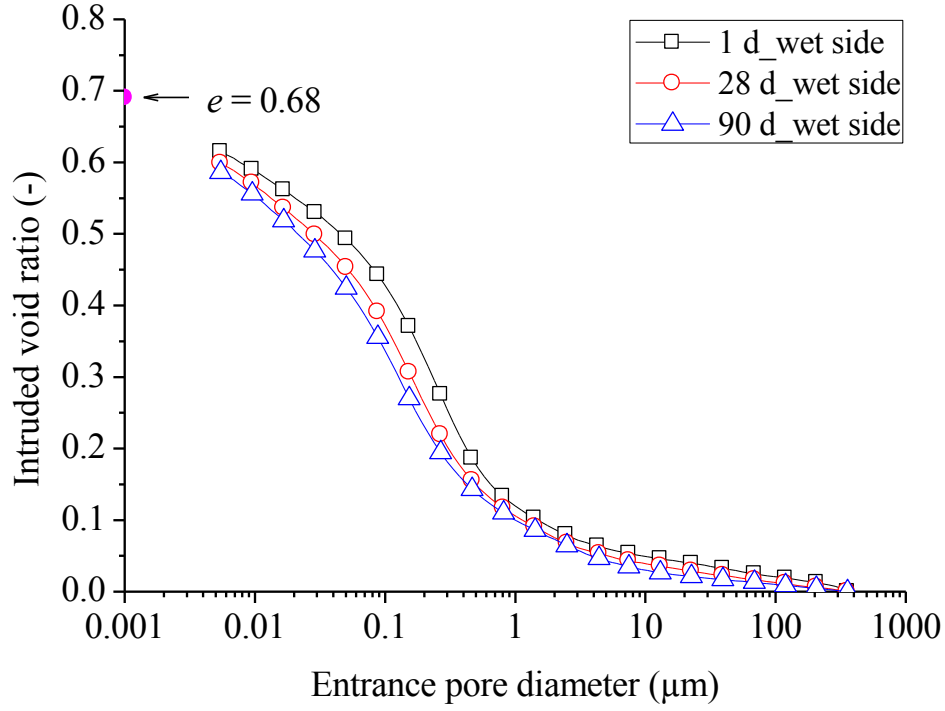

558

559 **Figure 7 (a) Derived pore size distribution curves of lime-treated sample compacted on the wet side and (b)**
560 **cumulative curves of lime-treated sample compacted on the wet side**

561

a)

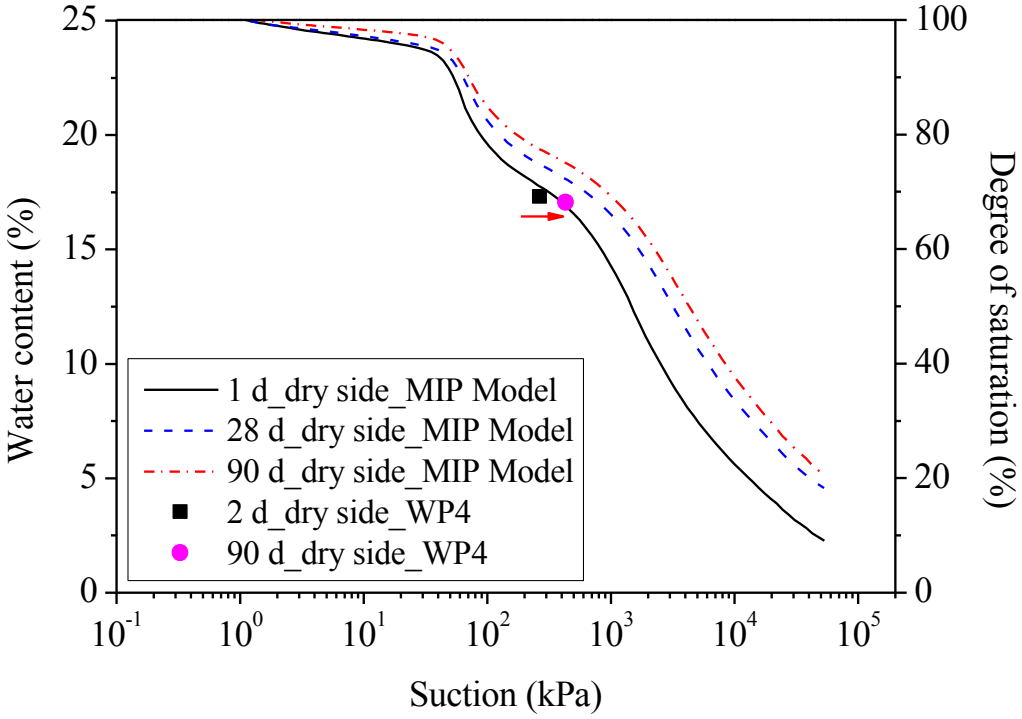

562

b)

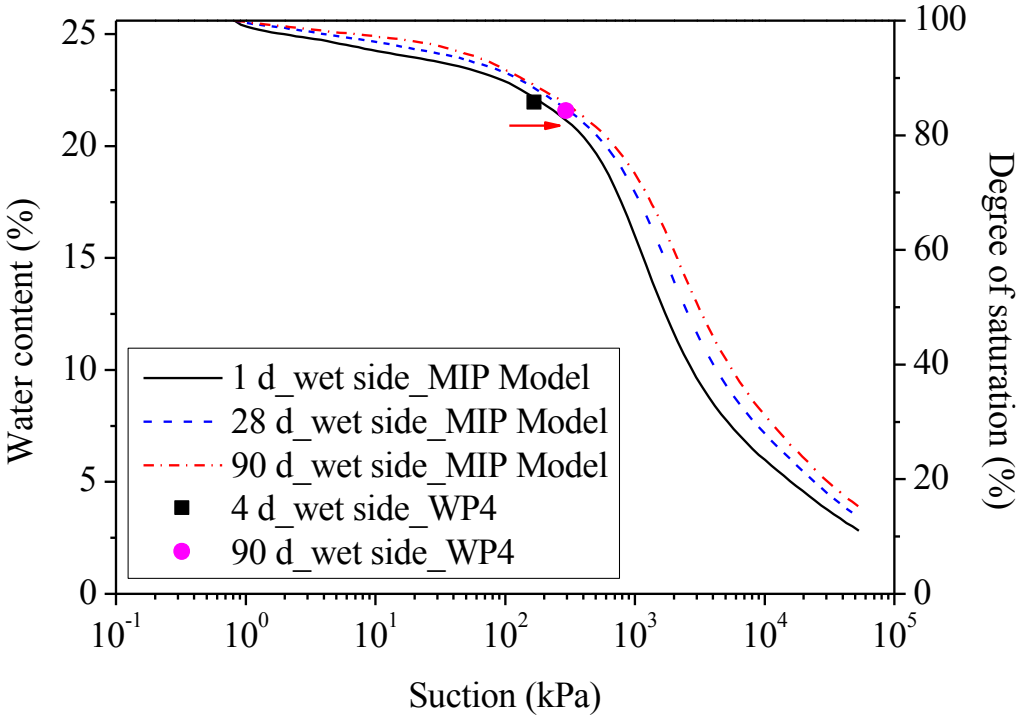

563

564 **Figure 8 Water retention curves of lime-treated silt determined from MIP data: (a) at dry side; (b) at wet**
565 **side**

566

567